

# Mesostructured MTES-Derived Silica Thin Film with Spherical Voids Investigated by TEM: 2. Dislocations and Strain Relaxation

X. Wu,<sup>†</sup> K. Yu,<sup>\*,‡</sup> C. J. Brinker,<sup>§</sup> and J. Ripmeester<sup>‡</sup>

*Institute for Microstructural Sciences, National Research Council of Canada, Ottawa, Ontario K1A 0R6, Canada, Steacie Institute for Molecular Sciences, National Research Council of Canada, Ottawa, Ontario K1A 0R6, Canada, and Sandia National Laboratories, MS 1349, Albuquerque, New Mexico 87185 and Center for Micro-Engineered Materials, University of New Mexico, Albuquerque, New Mexico 87131*

Received February 21, 2003. In Final Form: May 29, 2003

A mesostructured silica thin film with nanosized voids arranged in a body-centered cubic (bcc) array with a slight distortion was studied by transmission electron microscopy (TEM) for line defects. This film was engineered by a preferential solvent evaporation-induced sol-gel and self-assembly process and subsequent pyrolysis to remove its structure-directing agent. Methyl triethoxysilane [MTES, Si(OCH<sub>2</sub>-CH<sub>3</sub>)<sub>3</sub>CH<sub>3</sub>] was the silica precursor. Two types of dislocations were observed from a cross-sectional TEM sample of this non-free-standing film on a Si(001) substrate. One is an edge dislocation; the other is a dislocation dipole. The edge dislocation, with its Burgers vector  $\mathbf{b} = a[010]$  and dislocation line direction  $\xi = [100]$ , was formed by the reaction of two regular dislocations:  $\mathbf{b} = \mathbf{b}_1 + \mathbf{b}_2$ , while  $\mathbf{b}_1 = (a/2)[1, 1, -1]$  and  $\mathbf{b}_2 = (a/2)[-1, 1, 1]$ . The origin of this edge dislocation is related to the tensile strain developed in the film because of film shrinkage during the fabrication; its development is argued to arise from the partial relief of developed strain. A new concept, namely, critical mesostructure thickness for the occurrence of the stress relaxation, is proposed and computed using an elastic strain energy argument. The possible factors for the termination site of the edge dislocation are discussed briefly. The dislocation dipole has the Burgers vectors  $\mathbf{b} = \pm(a/2)[-1, 1, 1]$  on a (0, 1, -1) plane.

## 1. Introduction

The mesostructured porous silica thin film addressed in our transmission electron microscopy (TEM) study (part 1) is a special type of crystalline solid.<sup>1</sup> Similar to normal crystals, this mesostructured thin film has a three-dimensional order, but with a much larger lattice parameter ( $a \sim 13$  nm) than those (up to a few nanometers) observed in ordinary crystals. Instead of atoms (0.1–0.2 nm in diameter) in conventional crystals, nanometer-sized voids (ca. 4 nm in diameter) in the present ordered thin film are arranged in an ordered array and are distributed in the silica matrix, which is essentially amorphous. As was demonstrated in our TEM study part 1, this mesostructure has electron diffraction properties similar to those of ordinary crystals; however, a large TEM camera length ( $L = 2900$  mm) was required to obtain decipherable electron diffraction patterns because of its large lattice constant.<sup>1</sup> It is reasonable to expect that the present crystal has other physical properties, such as crystal defects, similar to those of traditional crystals.

It is generally acknowledged that crystals contain imperfections, the so-called defects. Defects, including point, line, surface, or volume defects, locally disturb the regular arrangement of atoms in ordinary crystals, and they have been studied extensively, especially line defects, which are also known as dislocations. Over the past few decades, studies on dislocations and their effects on the

mechanical properties of materials have advanced so much that a number of approaches have been put forward to resolve various problems.<sup>2–5</sup>

On the other hand, for mesostructured crystalline materials templated by amphiphiles, very little work has been performed on dislocations and the other defects, although the syntheses of these mesostructured porous materials have received great attention since 1992.<sup>6</sup> Defects in these materials should have special properties. Thus, it is essential to understand the fundamental mechanisms that govern the presence and development of the defects, to improve the experimental design leading to desirable products. Feng et al.<sup>7</sup> described TEM observations of two types of dislocations and two types of disclinations (namely, surface defects) in MCM-41, the first-reported mesostructured silica.<sup>6a</sup> This porous powder, with a two-dimensional hexagonal mesophase ( $p6mm$ ), was templated by a surfactant with silicate as the silica precursor. To the best of our knowledge, the study by Feng et al.<sup>7</sup> was the only one that reported on the defects in mesostructured porous materials. The two types of line defects observed were longitudinal edge dislocations and

(2) Hirth, J. P. *Acta Mater.* **2000**, *48*, 93.

(3) Wu, X.; Weatherly, G. C. *Philos. Mag. A* **2001**, *81*, 1489.

(4) (a) Matthews, J. W.; Blakeslee, A. E. *J. Cryst. Growth* **1974**, *27*, 118. (b) Matthews, J. W.; Blakeslee, A. E. *J. Cryst. Growth* **1975**, *29*, 273. (c) Matthews, J. W.; Blakeslee, A. E. *Thin Solid Films* **1976**, *33*, 253.

(5) (a) Hull, D. *Introduction to dislocation*; Pergamon Press: New York, 1968. (b) Grovenor, C. R. M. *Microelectronic Materials*; IOP Publishing, Ltd.: Bristol, England, 1989. (c) Hirth, J. P.; Loth, J.; *Theory of Dislocations*; Krieger: Melbourne, FL, 1992.

(6) (a) Kresge, C.; Leonowicz, M.; Roth, W.; Vartuli, C.; Beck, J. *Nature* **1992**, *359*, 710. (b) Ozin, G. A.; Chomski, E.; Khushalani, D.; MacLachlan, M. J. *Curr. Opin. Colloid Interface Sci.* **1998**, *3*, 181. (c) Brinker, C. J.; Lu, Y.; Sellinger, A.; Fan, H. *Adv. Mater.* **1999**, *11*, 579.

(7) Feng, J.; Huo, Q.; Petroff, P. M.; Stucky, G. D.; *Appl. Phys. Lett.* **1997**, *71*, 1887.

\* To whom correspondence should be addressed.

<sup>†</sup> Institute for Microstructural Sciences, National Research Council of Canada.

<sup>‡</sup> Steacie Institute for Molecular Sciences, National Research Council of Canada.

<sup>§</sup> Sandia National Laboratories and University of New Mexico.

(1) Yu, K.; Wu, X.; Brinker, C. J.; Ripmeester, J. *Langmuir* **2003**, *19*, 7282–7288.

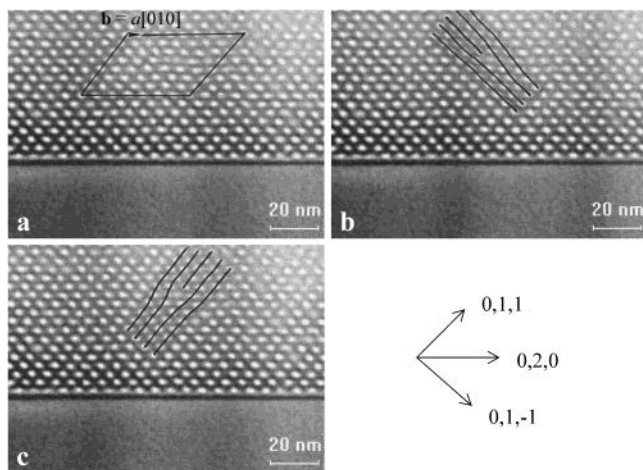


**Figure 1.** Bright-field TEM image of the cross-sectional sample along the [100] direction (a) with the Burgers circuit indicating the edge dislocation with  $\mathbf{b} = a[010]$ ; (b) with the guidance presenting the position of the extra (011) plane of dislocation  $\mathbf{b}_1 = (a/2)[1,1,-1]$ ; and (c) with the guidance explaining the position of the extra (0,1,-1) plane of dislocation  $\mathbf{b}_2 = (a/2)[-1,1,1]$ .  $\mathbf{b} = \mathbf{b}_1 + \mathbf{b}_2$ .

mixed dislocation dipoles, while the two types of surface defects were single  $+\pi$  disclinations and disclination quadrupoles. These defects observed are similar to those in liquid crystals and were suggested to form in the liquid-crystal-like stage before the silicate polymerization. It was acknowledged that these defects provided valuable information on the formation of the mesophase, although the causes for such defects were not dealt with.<sup>7</sup>

In the present study, we report on the TEM study of the dislocations in the mesostructured thin film with nano-sized voids organized in a body-centered cubic (bcc) array but with a slight distortion. The thin film was prepared via the so-called preferential solvent evaporation-induced sol-gel and self-assembly (EISGSA) process, which is quite different from that used to prepare MCM-41.<sup>6</sup> The description of the film synthesis and the preparation of the cross-sectional TEM sample can be found in part 1.<sup>1</sup> Two types of line defects were observed: edge dislocation and dislocation dipole. Shrinkage of the film during the fabrication of the mesostructure and the consequential strain ( $\epsilon \sim 3.7\%$ ) development and relaxation are argued to be the cause for the presence of the edge dislocation. A critical mesostructure thickness (CMST) for the presence of a dislocation is proposed, and the value is estimated theoretically using an elastic strain energy argument.<sup>3,4</sup> The elastic mismatch between the substrate and the thin film is also addressed.

## 2. Results and Discussion

The results and discussion section consists of three parts. The TEM observation of the line defects is presented in the first part. To understand the origin of the dislocation formation, the presence of strain due to film shrinkage during the fabrication is dealt with in the second part. The third part concerns the study of strain relaxation; both the CMST and the elastic mismatch between the silicon substrate and the sol-gel film are addressed. The CMST is based on the concept of critical film thickness (CFT) in semiconductor epitaxial films.<sup>3,4</sup>

**2.1. Dislocation Observations.** The mesostructure of the silica thin film prepared on a Si(001) substrate is not perfect, and line defects (dislocations) were observed. One example is presented in Figure 1a, which is a bright-field TEM image of the cross-sectional sample along the

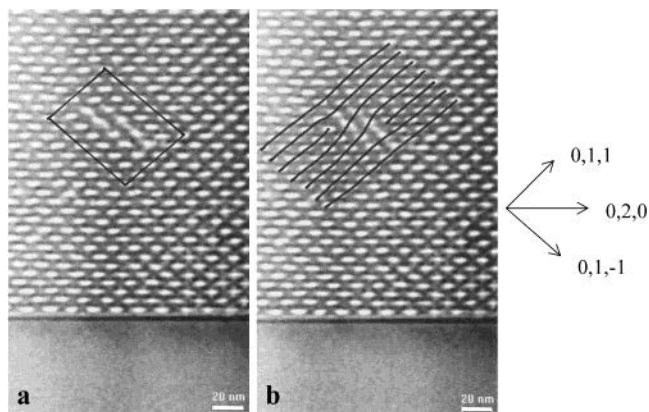
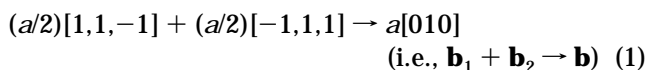


**Figure 2.** Bright-field TEM image of the cross-sectional sample along the [100] direction (a) with the Burgers circuit demonstrating the dislocation dipole with  $\mathbf{b} = 0$  and (b) with the guidance presenting the positions of the extra (0,1,-1) planes of individual dislocations  $\mathbf{b}_1$  and  $\mathbf{b}_2$ , namely,  $\pm(a/2)[-1,1,1]$ .

[100] zone axis. A Burgers circuit is constructed around the dislocation according to the finish to start, right-handed screw convention;<sup>5</sup> the Burgers vector of the dislocation is determined to be  $\mathbf{b} = a[010]$ . For typical bcc crystals, the Burgers vector of a unit slip dislocation should be  $(a/2)\langle 111 \rangle$ , while the slip plane is usually  $\{110\}$ ; thus, the usual slip systems are  $(a/2)\langle 111 \rangle - \{110\}$ . For the  $a[010]$  dislocation shown in Figure 1a, detailed analyses indicate that it was formed by the reaction of two regular bcc dislocations  $(a/2)\langle 111 \rangle$ , as is illustrated in Figure 1b,c. In Figure 1b, the dislocation with the Burgers vector  $\mathbf{b}_1 = (a/2)[1,1,-1]$  on slip plane (011) is indicated, and an extra (011) half plane (the middle line) is also indicated. As a result of the fact that the intersection of the slip plane (011) and surface (or interface) plane (001) is [100], the dislocation line direction is  $\xi_1 = [100]$ . This regular dislocation is a mixed type because the angle between  $\mathbf{b}_1$  and  $\xi_1$  is  $54.74^\circ$ . The other mixed-type dislocation is shown in Figure 1c, with the Burgers vector  $\mathbf{b}_2 = (a/2)[-1,1,1]$  and  $\xi_2 = [100]$  on the slip plane (0,1,-1); also, an extra (0,1,-1) half plane is indicated. When dislocations  $\mathbf{b}_1$  and  $\mathbf{b}_2$  meet at the intersection, they form the dislocation  $\mathbf{b}$  according to the reaction



According to reaction 1, the elastic strain energy of the dislocation decreases from  $3a^2/2$  to  $a^2$ . The  $a[010]$  dislocation shown in Figure 1a is an edge dislocation because its Burgers vector is normal to its line direction [100]. In conventional bcc crystals, the edge dislocation is typically stable and is usually immobile with respect to glide.<sup>5</sup>

Another type of dislocation examined is presented in Figure 2a, which is a bright-field TEM image of the cross-sectional sample along the zone axis [100]. A Burgers circuit is constructed around the defect region, and the Burgers vector of the dislocation shown in Figure 2a is 0. A detailed investigation reveals that this is a dislocation dipole.<sup>5</sup> As is demonstrated in Figure 2b, dislocations 1 and 2 are the same type but with opposite Burgers vectors, and they glide on the (0,1,-1) plane. The two extra half (0,1,-1) planes for the two dislocations ( $\mathbf{b}_1$  and  $\mathbf{b}_2$ ) are indicated also in Figure 2b. The Burgers vectors of the two dislocations are  $\pm(a/2)[-1,1,1]$ ; thus, the Burgers vector of the complete dipole is 0, as is shown in Figure 2a. According to the defect theories for traditional crystals, there are no long-range strain fields associated with the dipole.<sup>5</sup>

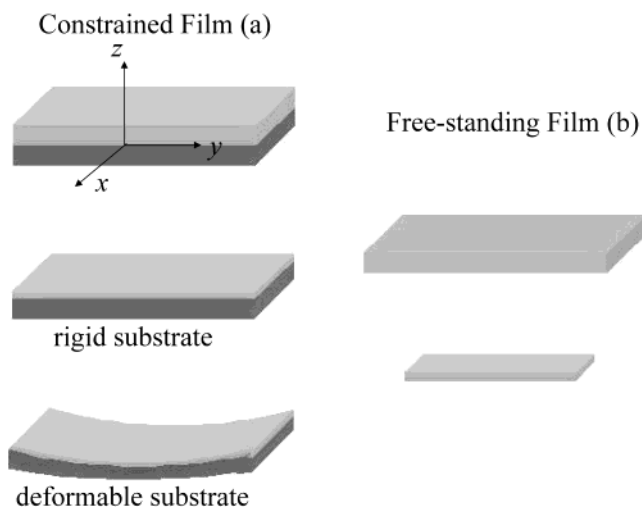


**Figure 3.** Schematic illustration of sol-gel thin films before and after the film shrinkage (after Lu).<sup>8a</sup> (a) The film shrinkage imposes a tensile stress in the non-free-standing film as well as a compressive stress in the substrate. (b) There is no residual stress left in the free-standing film.

### 2.2. Presence of Strain in the Mesostuctured Sol-Gel Film.

The present sol-gel silica thin film is non-free-standing and mesostructured with defects. Thus, a brief description of the gel network shrinkage and stress development during the common sol-gel fabrication is beneficial. It is acknowledged that the fabrication of sol-gel films involves solvent evaporation and gel network condensation during the drying process, as well as involves the removal of trapped solvent and further condensation during subsequent thermal treatment, such as pyrolysis.<sup>8-11</sup> Before the gel point is reached, the solvent evaporation is approximately the same as pure solvent evaporation. From the onset of gelation, stress develops as a result of the solvent evaporation, network condensation, and attachment of the film to a substrate. Many factors such as initial sol compositions, organic additives, and processing conditions, as well as the interplay between them, affect the stress developed in the drying process and the subsequent thermal treatment. In general, the drying and subsequent thermal treatment of the traditional sol-gel films are drastically complicated processes. During the two processes, the sol-gel films usually shrink. Consequently, biaxial tensile stresses develop in non-free-standing films that are constrained to substrates, due to the fact that the film shrinkage can only take place freely in the direction ( $z$ ) perpendicular to the film-substrate interface ( $x$ - $y$  plane). Thereby, such shrinkage imposes a tensile stress in the film as well as a compressive stress in the substrate (as is demonstrated in Figure 3a). On the other hand, if a sol-gel film (Figure 3b) is not attached to any substrate, there will be no such stress developed in the film because the film can shrink freely to its stress-free state.<sup>8-11</sup>

For the present mesoporous silica thin film on a Si substrate, the fabrication also involved solvent evaporation and network condensation during its drying process, as well as involved the removal of trapped solvent and further

condensation during subsequent pyrolysis. However, because of the presence of the structure-directing agent, namely, the amphiphilic polystyrene-*block*-poly(ethylene oxide) diblock copolymer in the initial sol,<sup>1</sup> the drying process and subsequent calcination process are even more complicated. It is easy to understand that the presence of the diblock copolymer should have an effect on both the physics and the chemistry of the two processes. The physical factors include the surface tension, contact angle, capillary pressure of the solvent, evaporation rate, and permeability and elastic modulus of the gel. The chemical factors include the rate and degree of siloxane condensation. Thus, it is problematical to give a quantitative or even qualitative illustration of the film shrinkage and the stress development, as well as their effects on the defect formation and evolution in the mesostructure. The self-assembly process was associated with drying in the EISGSA process, with an extensive period. Although imperfections could develop in both the stages of drying and those of calcination, we suspect that the dislocations observed in the present non-free-standing silica thin film were related to the drying process when the system was still fluidlike rather than to the pyrolysis;<sup>7</sup> the mesophase formation progressed faster than the film shrinkage as a result of the presence of the diblock copolymer. In addition, we argue that the edge dislocation was "locked in" after its formation.<sup>5</sup>

Furthermore, it seems reasonable to assume that all the strain that developed because of the film shrinkage was confined to the film, as was demonstrated in Figure 3a with a rigid substrate. This is due to the fact that the thickness of the film ( $h$ , ca. 300 nm) is several orders of magnitude smaller than that of the substrate ( $h_s$ , ca. 540  $\mu\text{m}$ ), as well as that the elastic modulus of the silicon substrate is much larger than that of the as-deposited silica thin film. Hence, the lattice constant of the bcc mesostructure changed from  $a_0$  to  $a_1$  before and after the film shrinkage, with  $a_0 > a_1$ . This change only took place in the  $z$  direction. Accordingly, the strain ( $\epsilon$ ) developed in the film can be expressed as

$$\epsilon = (a_0 - a_1)/a_0 \quad (2)$$

Because the mesostructure is characterized as body-centered tetragonal with  $a = 13.5$  nm and  $c = 13$  nm, which is slightly distorted from bcc with  $a = 13$  nm,<sup>1</sup> the strain  $\epsilon$  in the film is calculated using eq 2, and  $\epsilon = (13.5 - 13)/13.5 = 3.7\%$ . In a confined silica film but with a hexagonally packed arrangement of tubules, a deviation of 4% from perfect hexagonal was observed; hence, this slightly distorted hexagonal lattice was argued to encompass 4% strain, which was related to the polymerization of the inorganic phase.<sup>12</sup> That silica film is very much similar to the present one regarding its fabrication, where a dilute solution of the silica precursor, namely, tetraethoxysilane, was used to prevent homogeneous nucleation in the bulk solution and to promote heterogeneous nucleation and growth of the mesophase at its solution/substrate interface. For the present system, it is believed that the self-assembly started at the two interfaces, namely the liquid/substrate and liquid/gas interfaces, and progressed into the areas between the two interfaces.<sup>6c,13</sup>

(8) (a) Lu, M. C. Ph.D. Thesis, 2001, The University of New Mexico.

(b) Lu, M. C. Personal communication.

(9) (a) Scherer, G. W. *J. Non-Cryst. Solids*, **1987**, *89*, 217. (b) Scherer, G. W. *J. Non-Cryst. Solids*, **1989**, *109*, 171.

(10) Chen, K. S.; Schunk, R. P. *A one-dimensional analysis of sol-gel film-coating drying: pore evolution, network shrinkage and stress development*; Technical Report SAND; Sandia National Laboratory: 1998; pp i-iii, 1-24.

(11) Scherer, G. W. *J. Sol-Gel Sci. Technol.* **1997**, *8*, 353.

(12) Trau, M.; Yao, N.; Kim, E.; Xia, Y.; Whitesides, G. M.; Aksay, I. A. *Nature* **1997**, *390*, 674.

(13) Lu, Y.; Ganguli, R.; Drewien, C.; Anderson, M.; Brinker, C.; Gong, W.; Guo, Y.; Soyez, H.; Dunn, B.; Huang, M.; Zink, J. *Nature* **1997**, *389*, 364-368.



According to eq 1, this strain can also be recognized as the so-called misfit strain between the film and the substrate in semiconductor epitaxial films.<sup>2–5</sup> Because of its value (larger than 2%), the present system is a high-misfit system. In addition, the biaxial tensile stress in the film is a plane stress with  $\sigma_z = 0$ . Thereby, under the assumption of the absence of substrate bending, the biaxial tensile stress ( $\sigma$ ) in the film is calculated as

$$\sigma = \sigma_x = \sigma_y = \frac{Y}{1 - \nu^2}(\epsilon_x + \nu\epsilon_y) = 2\mu \frac{1 + \nu}{1 - \nu} \epsilon \quad (3)$$

where  $\epsilon_x = \epsilon_y = \epsilon$  and  $Y = 2\mu(1 + \nu)$ ,  $Y$  is the Young's modulus,  $\mu$  is the shear modulus, and  $\nu$  is the Poisson's ratio of the film.<sup>3</sup> For most materials,  $\nu = 0.3$ .<sup>14</sup>

It is known that the elastic modulus of typical microporous silica is exponentially proportional to its density. A high density implies that the degree of condensation of the gel network is high; thus, the modulus of the gel network is high. Therefore, the modulus reflects, to a certain extent, the rigidity of the gel. With the same porosity, mesostructured silica may, however, have a higher modulus than a nonstructured one.<sup>8</sup>

Because the present MTES-derived, mesostructured silica thin film with nanosized voids is a brand-new type of material, data on elastic properties are not available at present. Basically, it is hard to quantify the modulus until measurements become available. The modulus measurement of an as-cast thin film is almost impossible by traditional means such as indentation or simple tension test methods, although it is acknowledged that the modulus is an important parameter. For the bulk modulus ( $K$ ) of the present sol–gel film, its value must have changed from 0 to several GPa during its fabrication.<sup>8</sup> Before calcination, the bulk modulus is estimated to be 0.2–0.3 GPa and its Poisson's ratio ( $\nu$ ) to be 0.2; after calcination, the modulus is estimated to be 2–4 GPa. These estimates are based on the experimental data of similar thin films previously investigated.<sup>8</sup>

Although the drying stress is one of the most influential factors affecting the thin-film properties, only Lu has performed a preliminary study on the stress development in-situ during the sol–gel thin-film formation; the polysiloxane sols were derived from alkoxides.<sup>8</sup> The measured biaxial tensile stress ranged from almost 0 to several hundred MPa; both the magnitude and the development of the stress were dependent on the degree of the siloxane hydrolysis and condensation in the sol as well as the presence of additives. It was noticed that surfactant addition reduced the drying stress dramatically; however, there was no mesophase formation upon the presence of the surfactant, namely, cetyltrimethylammonium bromide [ $\text{CH}_3(\text{CH}_2)_{15}\text{N}^+(\text{CH}_3)_3\text{Br}^-$ ]. Accordingly, the effect of the mesophase formation on the drying stress is not available. As a result of the fact that the drying stress is reduced significantly by the amphiphile presence,<sup>8</sup> it seems reasonable that the mesostructure formed before considerable drying stress developed causes the shrinkage of the film.

After the shrinkage, the elastic strain energy per unit area ( $E$ ) in the present film with thickness  $h$  can be calculated as<sup>3</sup>

$$E = \frac{1}{2}\sigma_x\epsilon_x h + \frac{1}{2}\sigma_y\epsilon_y h = 2\mu \frac{1 + \nu}{1 - \nu} \epsilon^2 h \quad (4)$$

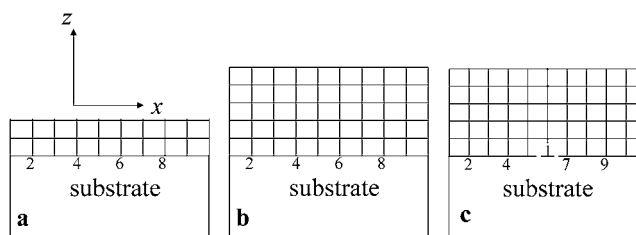


**Figure 4.** Schematic illustration of the plastic mechanism of the strain relaxation in a semiconductor epitaxial thin film (with the lattice planes sketched) on a rigid substrate. Before the film thickness reaches its CFT (a), the film is fully strained. When the film thickness reaches its CFT (b), the plastic relaxation takes place via the presence of a misfit dislocation and its development toward the film/substrate interface (c).

Equation 4 demonstrates that the strain energy of the film increases with increasing film thickness.

**2.3. Strain Relaxation.** It is helpful to mention that the mechanisms of the strain relaxation in semiconductor thin films, whose hetero-epitaxial growth, namely, lattice-mismatched growth, is achieved by techniques such as molecular-beam epitaxy, have been investigated comprehensively.<sup>3,4</sup> A semiconductor epitaxial film can be under tension or compression, when the lattice constant of the film is less or larger than that of its substrate, respectively. Because the present mesostructured thin film is under tension, a tensioned semiconductor epitaxial film is addressed. The concept of a CFT was first suggested by Matthews and Blakeslee:<sup>4</sup> a film is strained fully without the formation of defects to release the strain when the film thickness is below the critical thickness (Figure 4a); on the other hand, when the film thickness reaches the CFT or is larger than the CFT (Figure 4b), there is a driving force for the strain relaxation by the construction of defects (Figure 4c). The formation of dislocation to release the strain in the film is a plastic strain relaxation mechanism (Figure 4c), while the creation of surface instability is an elastic mechanism.<sup>15</sup> Also, cracking is another strain relaxation mechanism in tensile-strained films.<sup>16</sup>

As is demonstrated in Figure 4b, when the film is under tension, the lattice is stretched along the  $x$  (and  $y$ ) direction; thus, the strain (misfit) suggested by eq 2 becomes the origin of the elastic strain energy given by eq 4. This elastic strain energy can be reduced when an extra plane is introduced into the tensile-strained lattice, as is illustrated schematically in Figure 4c, as well as when the dislocation progresses toward the interface between the substrate and the film, so that the lattice is stretched less compared to that shown in Figure 4b. Consequently, a dislocation is formed at the CFT and afterward develops toward the film/substrate interface to release the strain. The Burgers vector of this dislocation (presented in Figure 4c) is  $a[100]$ , and the line direction is  $[010]$ , according to the Cartesian coordinate axes in Figure 4. This dislocation is an edge dislocation, and its Burgers vector  $a[100]$  should be 100% effective in relieving the strain in the film because  $a[100]$  is in the (001) surface (or interface) plane and is parallel to the lattice stretch direction  $x$  axis.

In general, when a dislocation is formed in a strained film (Figure 4c), the change in the elastic energy of the system can be given by

$$\Delta E = E_e + E_{\text{dis}} \quad (5)$$

(14) Dieter, D. E. *Mechanical Metallurgy*; McGraw-Hill: New York, 1988.

(15) (a) Srolovitz, D. J. *Acta Metall.* **1989**, *37*, 621. (b) Grilhe, J. *Acta Metall. Mater.* **1993**, *41*, 909.

(16) Wu, X.; Weatherly, G. C. *Acta Metall.* **1999**, *47*, 3383.

where  $E_e$  is the elastic energy relieved by the formation of the defect, while  $E_{\text{dis}}$  is the elastic energy associated with the dislocation presence.<sup>3</sup> The CFT ( $h_c$ ) for the formation of the defect can, thus, be obtained by solving the following equation:

$$\Delta E = 0 \quad (6)$$

The elastic energy per unit length relieved by the formation of one dislocation is given by

$$E_e = -\frac{2\mu(1+\nu)\epsilon hb \sin \beta \cos \varphi}{1-\nu} \quad (7)$$

where  $b$  is the magnitude of the dislocation Burgers vector,  $\beta$  is the angle between the Burgers vector and the dislocation line of the dislocation, and  $\varphi$  is the angle between the slip plane and the free surface (or interface).<sup>3</sup>

Meanwhile, the elastic energy per unit length associated with the dislocation can be characterized by

$$E_{\text{dis}} = \frac{\mu b^2(1-\nu \cos^2 \beta)}{4\pi(1-\nu)} \ln\left(\frac{2h}{r_0}\right) + \frac{\mu b^2 \sin^2 \beta}{8\pi(1-\nu)} \left[ \cos^2 \varphi - \sin^2 \varphi - \frac{1-2\nu}{2(1-\nu)} \right] + U_{\text{core}} \quad (8)$$

where  $r_0$  is the dislocation core radius and  $U_{\text{core}}$  is the energy per unit length of the dislocation core. Equation 8 is suitable for perfect dislocations; a stacking-fault energy should be considered additionally for partial dislocations, which are not dealt with in the present study.<sup>3</sup>

With Cottrell's approximation for the dislocation core energy,<sup>3,17</sup>

$$U_{\text{core}} = \frac{\mu b^2}{2\pi(1-\nu)^2} \quad (9)$$

substituting eqs 7 and 8 into 5 and solving eq 6, the CFT ( $h_c$ ) is, thereby, defined as

$$\frac{2(1+\nu)\epsilon h_c \sin \beta \cos \varphi}{1-\nu} = \frac{b(1-\nu \cos^2 \beta)}{4\pi(1-\nu)} \ln\left(\frac{2h}{r_0}\right) + \frac{b \sin^2 \beta}{8\pi(1-\nu)} \left[ \cos^2 \varphi - \sin^2 \varphi - \frac{1-2\nu}{2(1-\nu)} \right] + \frac{b}{2\pi(1-\nu)^2} \quad (10)$$

Equation 10 demonstrates that the value of the CFT, namely,  $h_c$ , is not a function of the shear modulus ( $\mu$ ) and, thus, not a function of any elastic modulus.

For the present sol-gel silica/diblock hybrid thin film, the growth mechanism is almost completely different from that of the semiconductor thin film. However, similarity can be deduced regarding the growth direction of the mesostructure. As was mentioned before, for the present system, it is believed that the self-assembly started at the two interfaces, namely, the solid/liquid and liquid/gas interfaces, and afterward progressed into the areas between the two interfaces.<sup>6c,13</sup> Consequently, the development of the mesostructure, along the direction ( $z$ ) perpendicular to the film/substrate interface ( $x$ - $y$  plane), is similar to the hetero-epitaxial growth of the semiconductor thin film, whose epitaxial growth is layer-by-layer from the substrate.

(17) Cottrell, A. H. *Dislocations and Plastic Flow in Crystal*; Oxford University Press: Oxford, 1953.

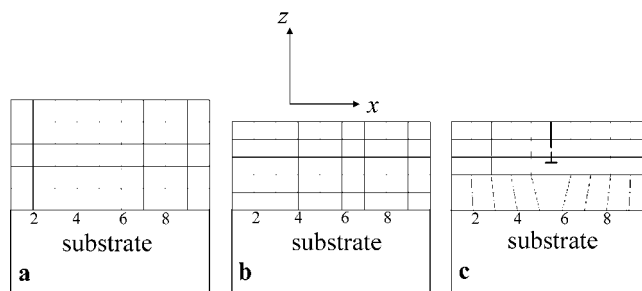


**Figure 5.** Schematic illustration of the strain relaxation via the plastic mechanism in the present mesostructured sol-gel film (with the lattice planes sketched) on the Si substrate. (a) The mesostructure constructed without significant film shrinkage, but (b) afterward with film shrinkage, the film can only contract freely in the direction ( $z$ ) perpendicular to the film/substrate interface ( $x$ - $y$  plane); (c) via the plastic relaxation, the strain is partly relieved in the constrained film by the formation of a dislocation and its development toward the film/substrate interface.

From now on, the film thickness is defined as the mesostructure thickness ( $h$ ). As was mentioned before, the physics and chemistry of the EISGSA fabrication is quite complicated, and it is impossible to correlate exactly the onset of mesophase formation and evolution<sup>18</sup> with the onset of the stress presence and film shrinkage. However, because of the amphiphile presence, we believe that the stress developed at the very late stage of the drying process;<sup>8</sup> therefore, the film shrinkage took place after the mesostructure formation, as was demonstrated in Figure 5. According to the CFT concept,<sup>3,4</sup> the strain relaxation might occur when the mesostructure thickness exceeded a critical value during the film shrinkage. This value is defined as the CMST.

In our CMST discussion, as a result of the fact that the edge dislocation in Figure 1a is the reaction production of the two regular dislocations shown in Figure 1b,c, we focus our attention on the one shown in Figure 1b. As was mentioned before, the Burgers vector  $a[100]$  of the edge dislocation indicated in Figure 4c should be 100% effective in relieving the strain in the film. However, for the regular dislocation presented in Figure 1b with the Burgers vector  $(a/2)[1,1,-1]$  on the (011) plane, only its edge component in the (001) plane can contribute to the strain relaxation, which is 57.7% of the total magnitude of the Burgers vector  $(a/2)[1,1,-1]$ . For this dislocation presented in Figure 1b, the magnitude of the Burgers vector  $|\mathbf{b}_1| = (\sqrt{3}/2)a = 11.26$  nm ( $a = 13$  nm),  $\beta = 54.74^\circ$ , and  $\varphi = 45^\circ$ .

Thus, plots of  $\Delta E$ ,  $E_e$ , and  $E_{\text{dis}}$ , versus the mesostructure thickness ( $h$ ; based on eqs 5 and 7–9) are presented in Figure 6. The shear modulus  $\mu$  used is 0.2 GPa and the Poisson's ratio  $\nu$  is 0.2.<sup>8,19</sup> Figure 6 demonstrates that, with the increase of  $h$ ,  $E_{\text{dis}}$  increases while  $E_e$  decreases; as a result, the total elastic energy change ( $\Delta E$ ) increases first; after  $\Delta E$  reaches a peak value, it decreases. After the mesostructure thickness exceeds  $h_c$ , the formation of dislocation is energetically favorable because  $\Delta E$  is  $<0$  and decreases more and more.

When the mesostructure thickness reaches a critical value ( $h_c$ ), which is the so-called CMST,  $\Delta E$  drops to 0. It was mentioned above that, theoretically, the value of the CMST can be obtained by solving eq 6,  $\Delta E = 0$ , and is

(18) Yu, K.; Drewien, C. A.; Brinker, C. J.; Hurd, A. J.; Eisenberg, A. *Mater. Res. Soc. Symp. Proc.* **2001**, 672, O8.15.

(19) This estimation of the shear modulus is based on the relationships:  $\mu = Y/[2(1+\nu)]$  and  $K = Y/[3(1-2\nu)]$ , where  $\mu$  is the shear modulus,  $K$  is the bulk modulus,  $Y$  is the Young's modulus, and  $\nu$  is the Poisson's ratio.

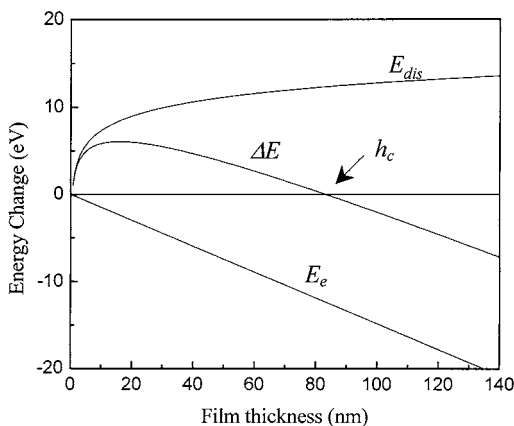


**Figure 6.** Plots of  $\Delta E$ ,  $E_e$ , and  $E_{dis}$  versus the mesostructure thickness ( $h$ ), regarding the dislocation (Figure 1b) observed in the mesostructured MTES-derived silica thin film with ordered voids, the tensile strain ( $\epsilon$ , misfit) of which is about 3.7%.

independent of the shear modulus ( $\mu$ ), as was demonstrated by eq 10. Here, the value of the CMST is  $h_c \sim 83$  nm, which is reasonable, compared with the film thickness (ca. 300 nm). It is noteworthy that the core site of the dislocation presented in Figure 1a is the termination site and not the site where it nucleated.

As is shown in Figure 1a, the location of the core of the edge dislocation is about 40 nm above the film/silicon interface; thus, it can be approximated as located at the third unit-cell layer (counting from the substrate toward the film with  $a = 13$  nm), as is illustrated in Figure 5c. As was mentioned before, this dislocation belongs to the so-called misfit dislocation. It is necessary to point out that in the classical approach, the so-called misfit dislocation, which compensates the strain between the substrate and the film, terminates usually at its equilibrium position, namely the film/substrate interface, as is shown in Figure 4c.<sup>4</sup> However, in the tensile-strained InGaAsP films on InP substrates, the misfit dislocations were found to be terminated usually inside the InP substrate rather than at the film/substrate interface; the elastic mismatch that exists between the harder InGaAsP film and the softer InP substrate was argued to cause such termination.<sup>3</sup> Accordingly, we argue that as a result of the fact that the shear modulus (64 GPa) of the silicon substrate is much larger than that of the film developed on this substrate, the misfit dislocation was slightly repelled away from the

interface and into the film. There might be other mechanisms, such as the dislocation being locked during its development by the siloxane condensation as well as the increase of the glass transition temperature ( $T_g$ ) of the polystyrene block during the preferential solvent evaporation, which prevent the misfit dislocation (Figure 1a) from reaching the film/substrate interface.<sup>20</sup>

For the dislocation dipole shown in Figure 2a, of the type the same as that observed in MCM41 powder,<sup>7</sup> we argue that it makes no contribution to the strain relaxation in the film. This argument is based on that, in typical crystals, there is only a local strain field associated with the dipole and the dipole has no effect on the strain field of the crystal.<sup>5</sup> Although the cause for the presence of the edge dislocation (shown in Figure 1a) may be strongly related to the film shrinkage in the EISGSA processes as well as the subsequent strain development and relaxation, the meaning of the formation of the dislocation dipole (shown in Figure 2a) is unclear.

### 3. Conclusions

Two types of dislocations in a MTES-derived silica thin film with ordered nanovoids were studied by TEM. One is an edge dislocation; the other is a dislocation dipole. The edge dislocation with the Burgers vector  $\mathbf{b} = a[010]$  was formed by the reaction of two normal dislocations:  $\mathbf{b}_1 = (a/2)[1, 1, -1]$  and  $\mathbf{b}_2 = (a/2)[-1, 1, 1]$ ; the cause for the formation is argued to partially relieve the tensile strain developed ( $\epsilon \sim 3.7\%$ ) during the film shrinkage in the fabrication process. With the help of an elastic strain energy argument, the concept of CMST for the formation of the dislocation was proposed and the CMST value was estimated theoretically. The calculated value is reasonable compared with the film thickness in the present study. A justification for the location of the edge dislocation is presented.

**Note Added after ASAP Posting.** This article was released ASAP on 8/6/2003 with a minor error in Figure 6. The correct version was posted 8/14/2003.

LA034309I

(20) (a) Zhang, L.; Yu, K.; Eisenberg, A. *Science* **1996**, *272*, 1777. (b) Yu, K.; Bartels, C.; Eisenberg, A. *Langmuir* **1999**, *15*, 7157. (c) Yu, K.; Hurd, A. J.; Eisenberg, A.; Brinker, C. J. *Langmuir* **2001**, *17*, 7961. (d) Yu, K.; Smarsly, B.; Brinker, C. J. *Adv. Funct. Mater.* **2003**, *13* (1), 47–52.